View metadata, citation and similar papers at core.ac.uk
brought to you by CORE
provided by Hochschulschriftenserver - Universität Frankfurt am Main

Identified Particle Elliptic Flow in Au + Au Collisions at $\sqrt{s_{NN}} = 130$ GeV

C. Adler,[11] Z. Ahammed,[23] C. Allgower,[12] J. Amonett,[14] B. D. Anderson,[14] M. Anderson,[5] G. S. Averichev,[9] J. Balewski,[12] O. Barannikova,[9,23] L. S. Barnby,[14] J. Baudot,[13] S. Bekele,[20] V. V. Belaga,[9] R. Bellwied,[30] J. Berger,[11] H. Bichsel,[29] L. C. Bland,[12] C. O. Blyth,[3] B. E. Bonner,[24] R. Bossingham,[15] A. Boucham,[26] A. Brandin,[18] R. V. Cadman,[1] H. Caines,[20] M. Calderón de la Barca Sánchez,[31] A. Cardenas,[23] J. Carroll,[15] J. Castillo,[26] M. Castro,[30] D. Cebra,[5] S. Chattopadhyay,[30] M. L. Chen,[2] Y. Chen,[6] S. P. Chernenko,[9] M. Cherney,[8] A. Chikanian,[31] B. Choi,[27] W. Christie,[2] J. P. Coffin,[13] L. Conin,[26] T. M. Cormier,[30] J. G. Cramer,[29] H. J. Crawford,[4] M. DeMello,[24] W. S. Deng,[14] A. A. Derevschikov,[22] L. Didenko,[2] J. E. Draper,[5] V. B. Dunin,[9] J. C. Dunlop,[31] V. Eckardt,[16] L. G. Efimov,[9] V. Emelianov,[18] J. Engelage,[4] G. Eppley,[24] B. Erazmus,[26] P. Fachini,[25] E. Finch,[31] Y. Fisyak,[2] D. Flierl,[11] K. J. Foley,[2] J. Fu,[15] N. Gagunashvili,[9] J. Gans,[31] L. Gaudichet,[26] M. Germain,[13] F. Geurts,[24] V. Ghazikhanian,[6] J. Grabski,[28] O. Grachov,[30] D. Greiner,[15] V. Grigoriev,[18] M. Guedon,[13] E. Gushin,[18] T. J. Hallman,[2] D. Hardtke,[15] J. W. Harris,[31] M. Heffner,[5] S. Heppelmann,[21] T. Herston,[23] B. Hippolyte,[13] A. Hirsch,[23] E. Hjort,[15] G. W. Hoffmann,[27] M. Horsley,[31] H. Z. Huang,[6] T. J. Humanic,[20] H. Hümmler,[16] G. Igo,[6] A. Ishihara,[27] Yu. I. Ivanshin,[10] P. Jacobs,[15] W. W. Jacobs,[12] M. Janik,[28] I. Johnson,[15] P. G. Jones,[3] E. Judd,[4] M. Kaneta,[15] M. Kaplan,[7] D. Keane,[14] A. Kisiel,[28] J. Klay,[5] S. R. Klein,[15] A. Klyachko,[12] A. S. Konstantinov,[22] L. Kotchenda,[18] A. D. Kovalenko,[9] M. Kramer,[19] P. Kravtsov,[18] K. Krueger,[1] C. Kuhn,[13] A. I. Kulikov,[9] G. J. Kunde,[31] C. L. Kunz,[7] R. Kh. Kutuev,[10] A. A. Kuznetsov,[9] L. Lakehal-Ayat,[26] J. Lamas-Valverde,[24] M. A. C. Lamont,[3] J. M. Landgraf,[2] S. Lange,[11] C. P. Lansdell,[27] B. Lasiuk,[31] F. Laue,[2] A. Lebedev,[2] T. LeCompte,[1] R. Lednický,[9] V. M. Leontiev,[22] P. Leszczynski,[28] M. J. LeVine,[2] Q. Li,[30] Q. Li,[15] S. J. Lindenbaum,[19] M. A. Lisa,[20] T. Ljubicic,[2] W. J. Llope,[24] G. LoCurto,[16] H. Long,[6] R. S. Longacre,[2] M. Lopez-Noriega,[20] W. A. Love,[2] D. Lynn,[2] R. Majka,[31] A. Maliszewski,[28] S. Margetis,[14] L. Martin,[26] J. Marx,[15] H. S. Matis,[15] Yu. A. Matulenko,[22] T. S. McShane,[8] F. Meissner,[15] Yu. Melnick,[22] A. Meschanin,[22] M. Messer,[2] M. L. Miller,[31] Z. Milosevich,[7] N. G. Minaev,[22] J. Mitchell,[24] V. A. Moiseenko,[10] D. Moltz,[15] C. F. Moore,[27] V. Morozov,[15] M. M. de Moura,[30] M. G. Munhoz,[25] G. S. Mutchler,[24] J. M. Nelson,[3] P. Nevski,[2] V. A. Nikitin,[10] L. V. Nogach,[22] B. Norman,[14] S. B. Nurushev,[22] G. Odyniec,[15] A. Ogawa,[21] V. Okorokov,[18] M. Oldenburg,[16] D. Olson,[15] G. Paic,[20] S. U. Pandey,[30] Y. Panebratsev,[9] S. Y. Panitkin,[2] A. I. Pavlinov,[30] T. Pawlak,[28] V. Perevoztchikov,[2] W. Peryt,[28] V. A. Petrov,[10] W. Pinganaud,[26] E. Platner,[24] J. Pluta,[28] N. Porile,[23] J. Porter,[2] A. M. Poskanzer,[15] E. Potrebenikova,[9] D. Prindle,[29] C. Pruneau,[30] S. Radomski,[28] G. Rai,[15] O. Ravel,[26] R. L. Ray,[27] S. V. Razin,[9,12] D. Reichhold,[8] J. G. Reid,[29] F. Retiere,[15] A. Ridiger,[18] H. G. Ritter,[15] J. B. Roberts,[24] O. V. Rogachevski,[9] J. L. Romero,[5] C. Roy,[26] D. Russ,[7] V. Rykov,[30] I. Sakrejda,[15] J. Sandweiss,[31] A. C. Saulys,[2] I. Savin,[10] J. Schambach,[27] R. P. Scharenberg,[23] K. Schweda,[15] N. Schmitz,[16] L. S. Schroeder,[15] A. Schüttauf,[16] J. Seger,[8] D. Seliverstov,[18] P. Seyboth,[16] E. Shahaliev,[9] K. E. Shestermanov,[22] S. S. Shimanskii,[9] V. S. Shvetcov,[10] G. Skoro,[9] N. Smirnov,[31] R. Snellings,[15] J. Sowinski,[12] H. M. Spinka,[1] B. Srivastava,[23] E. J. Stephenson,[12] R. Stock,[11] A. Stolpovsky,[30] M. Strikhanov,[18] B. Stringfellow,[23] H. Stroebele,[11] C. Struck,[11] A. A. P. Suaide,[30] E. Sugarbaker,[20] C. Suire,[13] M. Šumbera,[9] T. J. M. Symons,[15] A. Szanto de Toledo,[25] P. Szarwas,[28] J. Takahashi,[25] A. H. Tang,[14] J. H. Thomas,[15] V. Tikhomirov,[18] T. A. Trainor,[29] S. Trentalange,[6] M. Tokarev,[9] M. B. Tonjes,[17] V. Trofimov,[18] O. Tsai,[6] K. Turner,[2] T. Ullrich,[2] D. G. Underwood,[1] G. Van Buren,[2] A. M. VanderMolen,[17] A. Vanyashin,[15] I. M. Vasilevski,[10] A. N. Vasiliev,[22] S. E. Vigdor,[12] S. A. Voloshin,[30] F. Wang,[23] H. Ward,[27] J. W. Watson,[14] R. Wells,[20] T. Wenaus,[2] G. D. Westfall,[17] C. Whitten, Jr.,[6] H. Wieman,[15] R. Willson,[20] S. W. Wissink,[12] R. Witt,[14] N. Xu,[15] Z. Xu,[31] A. E. Yakutin,[22] E. Yamamoto,[6] J. Yang,[6] P. Yepes,[24] A. Yokosawa,[1] V. I. Yurevich,[9] Y. V. Zanevski,[9] I. Zborovský,[9] W. M. Zhang,[14] R. Zoulkarneev,[10] and A. N. Zubarev[9]

(STAR Collaboration)

[1]*Argonne National Laboratory, Argonne, Illinois 60439*
[2]*Brookhaven National Laboratory, Upton, New York 11973*
[3]*University of Birmingham, Birmingham, United Kingdom*
[4]*University of California, Berkeley, California 94720*
[5]*University of California, Davis, California 95616*
[6]*University of California, Los Angeles, California 90095*
[7]*Carnegie Mellon University, Pittsburgh, Pennsylvania 15213*
[8]*Creighton University, Omaha, Nebraska 68178*
[9]*Laboratory for High Energy (JINR), Dubna, Russia*
[10]*Particle Physics Laboratory (JINR), Dubna, Russia*

 0031-9007/01/87(18)/182301(6)$15.00 © 2001 The American Physical Society

[11]*University of Frankfurt, Frankfurt, Germany*
[12]*Indiana University, Bloomington, Indiana 47408*
[13]*Institut de Recherches Subatomiques, Strasbourg, France*
[14]*Kent State University, Kent, Ohio 44242*
[15]*Lawrence Berkeley National Laboratory, Berkeley, California 94720*
[16]*Max-Planck-Institut fuer Physik, Munich, Germany*
[17]*Michigan State University, East Lansing, Michigan 48824*
[18]*Moscow Engineering Physics Institute, Moscow, Russia*
[19]*City College of New York, New York City, New York 10031*
[20]*The Ohio State University, Columbus, Ohio 43210*
[21]*Pennsylvania State University, University Park, Pennsylvania 16802*
[22]*Institute of High Energy Physics, Protvino, Russia*
[23]*Purdue University, West Lafayette, Indiana 47907*
[24]*Rice University, Houston, Texas 77251*
[25]*Universidade de Sao Paulo, Sao Paulo, Brazil*
[26]*SUBATECH, Nantes, France*
[27]*University of Texas, Austin, Texas 78712*
[28]*Warsaw University of Technology, Warsaw, Poland*
[29]*University of Washington, Seattle, Washington 98195*
[30]*Wayne State University, Detroit, Michigan 48201*
[31]*Yale University, New Haven, Connecticut 06520*
(Received 5 July 2001; published 10 October 2001)

We report first results on elliptic flow of identified particles at midrapidity in Au + Au collisions at $\sqrt{s_{NN}} = 130$ GeV using the STAR TPC at RHIC. The elliptic flow as a function of transverse momentum and centrality differs significantly for particles of different masses. This dependence can be accounted for in hydrodynamic models, indicating that the system created shows a behavior consistent with collective hydrodynamical flow. The fit to the data with a simple model gives information on the temperature and flow velocities at freeze-out.

DOI: 10.1103/PhysRevLett.87.182301 PACS numbers: 25.75.Ld

The goal of the ultrarelativistic nuclear collision program is the creation of a system of deconfined quarks and gluons [1]. The azimuthal anisotropy of the transverse momentum distribution for noncentral collisions is thought to be sensitive to the early evolution of the system [2]. The second Fourier coefficient of this anisotropy, v_2, is called elliptic flow. It is an important observable since it is sensitive to the rescattering of the constituents in the created hot and dense matter. This rescattering converts the initial spatial anisotropy, due to the almond shape of the overlap region of noncentral collisions, into momentum anisotropy. The spatial anisotropy is largest early in the evolution of the collision, but as the system expands and becomes more spherical, this driving force quenches itself. Therefore, the magnitude of the observed elliptic flow should reflect the extent of the rescattering at relatively early time [2].

Elliptic flow in ultrarelativistic nuclear collisions was first discussed in Ref. [3] and has been studied intensively in recent years at the Alternating Gradient Synchrotron (AGS) [4,5], at the Super Proton Synchrotron (SPS) [6–8], and at the Relativistic Heavy Ion Collider (RHIC) [9] energies. The studies at top AGS energy and SPS have found that elliptic flow at these energies is in the plane defined by the beam direction and the impact parameter, $v_2 > 0$, as expected from most models. The pion elliptic flow for relatively peripheral collisions increases with beam energy [10] from about 0.02 at the top AGS energy [4], 0.035 at the SPS [7] to about 0.06 at RHIC energies [9]. The increased magnitude of the integrated elliptic flow at RHIC reaches the values predicted by hydrodynamical models, which are based on the assumption of complete local thermalization.

The first elliptic flow results from RHIC were for charged particles. The differential charged particle flow, $v_2(p_t)$, shows an almost linear rise with transverse momentum, p_t, up to 1.5 GeV/c. At $p_t > 1.5$ GeV/c, the $v_2(p_t)$ values start to saturate, which might indicate the onset of hard processes [9,11–13]. The behavior of $v_2(p_t)$ up to 1.5 GeV/c is consistent with a hydrodynamic picture. Hydrodynamics assumes complete local thermalization at the formation of the system, followed by an evolution governed by an equation of state (EOS). However, the p_t-integrated elliptic flow, v_2, as a function of centrality, and the differential $v_2(p_t)$, show little sensitivity to the EOS used [14]. Studies of the mass dependences of elliptic flow for particles with $p_t <$ 1.5 GeV/c provide important additional tests of the hydrodynamical model [15]. Similar to the identified single particle spectra, where the transverse flow velocity has been extracted from the mass dependence of the slope parameter [16], the $v_2(p_t)$ for different mass particles allows the extraction of the elliptic component of the flow velocity [17,18]. Moreover, the details of the dependence of elliptic flow on particle mass and transverse momentum

are sensitive to the temperature, transverse flow velocity, its azimuthal variation, and source deformation at freeze-out. In this Letter we report the first results for identified particle $v_2(m, p_t)$ in Au + Au collisions at RHIC at $\sqrt{s_{NN}} = 130$ GeV.

The Solenoidal Tracker At RHIC (STAR) [19], is ideally suited for measuring elliptic flow due to its azimuthal symmetry and large coverage. The detector consists of several subsystems in a large solenoidal magnet. The time projection chamber (TPC) covers the pseudorapidity range $|\eta| < 1.8$ for collisions in the center of the TPC. The magnet was operated at a 0.25 T field, allowing tracking of particles with $p_t > 75$ MeV/c. Two zero degree calorimeters [20] located at $|\sin\theta| < 0.002$, which mainly detect fragmentation neutrons, are used in coincidence for the trigger. The TPC is surrounded by a scintillator barrel which measures the charged particle multiplicity within $|\eta| < 1$, for triggering purposes.

For this analysis, 120 000 minimum-bias events were selected with a primary vertex position within 75 cm longitudinally of the TPC center and within 1 cm radially of the beam line. For determination of the event plane [9], charged particle tracks were selected with $0.1 < p_t \leq 2.0$ GeV/c. All tracks used in this analysis passed within 2 cm of the primary vertex and had at least 15 measured space points. Also, the ratio of the number of measured space points to the expected maximum number of space points for that particular track was required to be greater than 0.52, suppressing split tracks from being counted more than once. The tracks used for the determination of the reaction plane were within $|\eta| < 1.0$, and the tracks used to calculate the elliptic flow were within $|\eta| < 1.3$. These cuts are similar to the ones used in Ref. [9], and the analysis results presented here are not sensitive to those cuts.

The pions, protons, and antiprotons were selected according to their specific energy loss (dE/dx) in the TPC in the transverse momentum range of 0.175–0.75 GeV/c, 0.5–0.9 GeV/c, and 0.3–0.9 GeV/c, respectively. The lower p_t values were chosen such that the energy loss in the detector was negligible. At low momentum, the proton background due to secondary interactions with the detector material is significant. Therefore, only protons above a transverse momentum of 0.5 GeV/c were used in this analysis. At a momentum (p) of 0.5 GeV/c, the dE/dx resolution was found to be of the order of 11% for a typical long track in the STAR TPC. The kaons, because of their overlap in dE/dx with the electrons and positrons, were selected in the momentum ranges of 0.30–0.40 GeV/c and 0.60–0.70 GeV/c. The raw yields of the pions, kaons, protons, and antiprotons were obtained from fitting the dE/dx distributions for each η, p, and centrality bin with multiple Gaussians, and requiring greater than 90% purity (particle's yield divided by the sum of yields for all particles at that same dE/dx). Figure 1 shows the dE/dx distributions for negative tracks in the TPC for central events

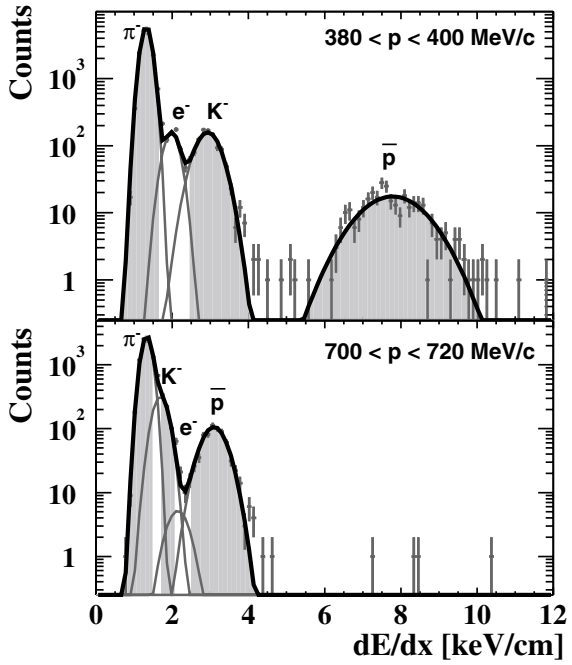

FIG. 1. Charged particle identification for central events at $|\eta| \leq 0.1$ for the momentum range of 380–400 MeV/c and 700–720 MeV/c. The shaded areas show the selected ranges for the different particles.

and $|\eta| \leq 0.1$. The upper panel shows the dE/dx distribution for the momentum range of 0.38–0.40 GeV/c and the multiple Gaussian fit. In this momentum range, the π^-, e^-, K^-, and $\bar{p}$ are clearly separated. The lower panel shows the dE/dx distribution for the momentum range of 0.70–0.72 GeV/c. For the higher momentum bin, the π^-, e^-, and K^- overlap; however, the $\bar{p}$ is still clearly separated. Even though it is still possible to extract kaons with 90% purity in this momentum bin, we used only the kaons up to 0.70 GeV/c.

The flow analysis method [21] involves the calculation of the event plane angle, which is an experimental estimator of the real reaction-plane angle. For the analysis presented in this Letter, each particle was correlated with the event plane from all the other particles (for the other methods, see [22]). The differential elliptic flow, v_2, depends on mass, rapidity (y), and p_t. In Fig. 2, $v_2(p_t)$ is shown for pions, kaons, and protons + antiprotons for minimum-bias collisions [23], integrated over rapidity and centrality by taking the multiplicity-weighted average. The uncertainties shown are statistical only. Using the same procedure to estimate the systematic uncertainties as in Ref. [9] for v_2 integrated over p_t, the systematic uncertainty for minimum-bias data is 13%. We have verified that the positive and negative identified particles used in this analysis have the same $v_2(p_t)$ within statistical uncertainties. For $v_2(p_t)$, the pions were integrated over $|y| \leq 1.0$, the kaons over $|y| \leq 0.8$, and the protons + antiprotons over $|y| \leq 0.5$ (the rapidity ranges chosen correspond to approximately consistent $|\eta|$ coverage for all of the

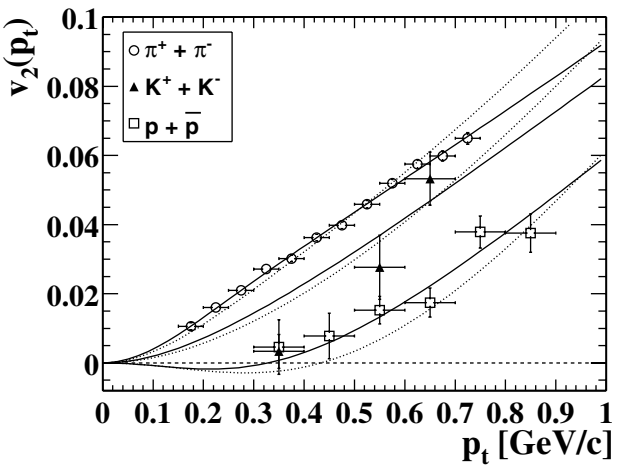

FIG. 2. Differential elliptic flow for pions, kaons, and protons + antiprotons for minimum-bias events. The solid lines show the fit with the modified blast wave model, and the dotted lines are the fit with the unmodified model.

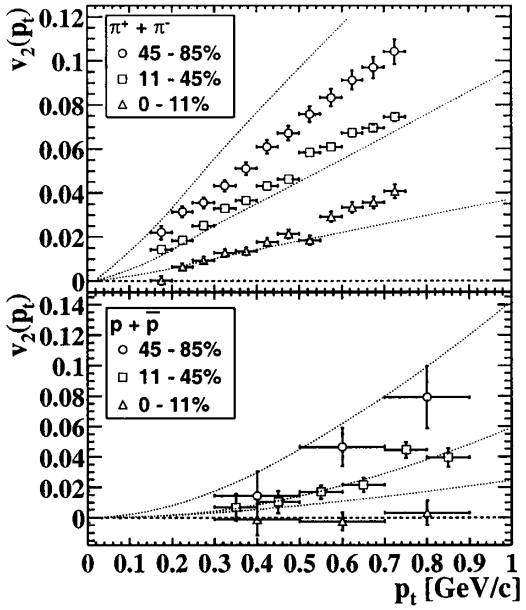

FIG. 3. Upper panel: Differential elliptic flow for pions in three different centrality bins. Lower panel: The same for protons + antiprotons. The dotted lines show the predictions from a full hydrodynamic model calculation [15]. The uncertainties shown are statistical only.

selected particles). Mathematically the v_2 value at $p_t = 0$, as well as its first derivative, must be zero. As a function of p_t, the pions exhibit an almost linear dependence of v_2, whereas the protons + antiprotons exhibit a more quadratic behavior, clearly different from the pions. As expected in a hydrodynamic picture, the kaons lie between the pions and the protons + antiprotons. The 90% purity of the protons + antiprotons in the $0.8 \leq p_t \leq 0.9$ range leads to a maximum +5% systematic error on the v_2 value in this bin. The observed behavior may be the result of the interplay between the mean expansion velocity, the elliptic component of the expansion velocity, and the thermal velocity of the particles. A similar effect was discussed for the case of directed flow in [24].

The differential elliptic flow, $v_2(p_t)$, is plotted for pions for three different centrality selections in the upper panel of Fig. 3, and for protons in the lower panel. The open triangles represent the most central 11% of the measured cross section. The open squares correspond to 11%–45% of the measured cross section, and the open circles correspond to 45%–85%. The uncertainties on the points are statistical only. The systematic uncertainty is smallest for the centrality region with the best reaction plane resolution and is estimated to be 20% for the most central bin, 8% for the midcentral bin, and 22% for the most peripheral bin. At a given p_t, the more peripheral collisions have the largest value of $v_2(p_t)$, and $v_2(p_t)$ decreases for more central collisions. For all three of the centrality ranges, in the measured p_t range, the p_t dependence of v_2 for pions is approximately linear.

We have fitted the data with a simple hydrodynamic-motivated model. This model is a generalization of the blast wave model from [15,25] assuming the flow field is perpendicular to the freeze-out hypersurface.

$$v_2(p_t) = \frac{\int_0^{2\pi} d\phi_b \cos(2\phi_b) I_2(\alpha_t) K_1(\beta_t)[1 + 2s_2 \cos(2\phi_b)]}{\int_0^{2\pi} d\phi_b I_0(\alpha_t) K_1(\beta_t)[1 + 2s_2 \cos(2\phi_b)]}, \quad (1)$$

where I_0, I_2, and K_1 are modified Bessel functions, and where $\alpha_t(\phi_b) = (p_t/T_f)\sinh(\rho(\phi_b))$, and $\beta_t(\phi_b) = (m_t/T_f)\cosh(\rho(\phi_b))$. The basic assumptions of this model are boost-invariant longitudinal expansion and freeze-out at constant temperature T_f on a thin shell, which expands with a transverse rapidity exhibiting a second harmonic azimuthal modulation given by $\rho(\phi_b) = \rho_0 + \rho_a \cos(2\phi_b)$. In this equation, ϕ_b is the azimuthal angle (measured with respect to the reaction plane) of the boost of the source element on the freeze-out hypersurface [15], and ρ_0 and ρ_a are the mean transverse expansion rapidity [$v_0 = \tanh(\rho_0)$] and the amplitude of its azimuthal variation, respectively. With $s_2 = 0$, our equation reduces to Eq. (2) from [15]. In Fig. 2, the fit to the minimum-bias data with $s_2 = 0$ is shown as the dotted lines. The poor fit shows that the data cannot be described under the assumption of a spatially isotropic freeze-out hypersurface in the transverse plane. This led us to generalize Eq. (2) from [15] to the case of a spatially anisotropic freeze-out hypersurface, introducing one extra parameter, s_2, describing the variation in the azimuthal density of the source elements, $\propto 2s_2 \cos(2\phi_b)$. This additional parameter leads to a good description of the data, shown as the solid lines in Fig. 2. A positive value of the s_2 parameter would mean that there are more source elements

moving in the direction of the reaction plane. The s_2 parameter does not distinguish between an in-plane or an out-of-plane extended source, because the direction of the flow field is not an observable. However, azimuthally sensitive Hanbury Brown-Twist measurements will be able to address this. In this model [Eq. (1)], elliptic flow as a function of particle transverse momentum, $v_2(p_t)$, starts from zero and rises approximately quadratically with p_t until the particle becomes relativistic, and then $v_2(p_t)$ continues to rise almost linearly. For the heavier particles, the linear rise is delayed. These mass-dependent effects are larger for lower temperatures (T_f) and larger transverse rapidities (ρ_0). The linear rise increases with both the amplitude of the azimuthal variation of the transverse expansion rapidity (ρ_a) and the elliptic deformation (s_2), but only ρ_a produces a mass dependence. This arises from the dependence of the s_2 parameter effect on momentum not energy. This also results in a change in slope and a characteristic curvature in $v_2(p_t)$, since the flow associated with s_2 saturates quite early, when $p_t/T \gg 1$ [26]. The fact that the data cannot be described with $s_2 = 0$ leads to the interpretation that the elliptic flow is not caused by an azimuthal velocity variation alone, but by the combination of a velocity difference and a spatially anisotropic freeze-out hypersurface.

Table I lists the results of the two fits (without and with s_2) for minimum-bias data. The parameters are correlated and therefore have large uncertainties. It is expected that better constraints on the parameters can be obtained in the future, when the fits to the single inclusive spectra for different mass particles are available. As the solid lines in Fig. 2 show, the data could be described by a reasonable set of parameters. For the different centralities, the T_f and ρ_0 were kept fixed to the minimum-bias values. Both the obtained ρ_a and s_2, not shown, decrease from peripheral to central collisions as expected from a simple geometrical picture.

A full hydrodynamic calculation, shown in Ref. [15], describes the $v_2(p_t)$ for pions, kaons, and protons + antiprotons for minimum-bias collisions equally well. The agreement is consistent with early local thermal equilibrium and the presence of an early stage pressure gradient. However, within the current statistical uncertainties in the data and different theoretical interpretations [27], the measurement does not justify drawing inferences about the different EOS. Comparing the centrality dependence from our Fig. 3 with the same hydrodynamic calculation shows a deviation which is most pronounced for the most peripheral data. This might indicate that the amount of particle rescattering in peripheral collisions is insufficient to justify the local thermal approximation implicit in hydrodynamical models.

TABLE I. The parameters from the blast wave fit for minimum-bias collisions. The first row lists the parameters for the unmodified fit ($s_2 = 0$), the second row gives the results from the fit function including the spatially anisotropic freeze-out hypersurface.

T_f (MeV)	ρ_0	ρ_a	s_2
135 ± 19	0.58 ± 0.03	0.09 ± 0.02	0
101 ± 24	0.61 ± 0.05	0.04 ± 0.01	0.04 ± 0.01

We have made the first measurement of identified particle elliptic flow at RHIC. The measured elliptic flow as a function of p_t and centrality differs significantly for particles of different masses. This mass dependence can be described with a simple hydrodynamic-motivated blast wave model. This model suggests that elliptic flow is generated by the combination of an azimuthal velocity variation and a spatially anisotropic freeze-out hypersurface. The mass dependence of $v_2(p_t)$ is also in close agreement with full hydrodynamic model calculations, suggesting that in Au + Au collisions at $\sqrt{s_{NN}} = 130$ GeV, a system is created which, for central and midperipheral collisions, is consistent with early local thermal equilibrium followed by hydrodynamic expansion.

We thank P. Huovinen for providing us with the hydrodynamical model calculation, the RHIC Operations Group at Brookhaven National Laboratory for their tremendous support and for providing collisions for the experiment. This work was supported by the Division of Nuclear Physics and the Division of High Energy Physics of the Office of Science of the U.S. Department of Energy, the United States National Science Foundation, the Bundesministerium für Bildung und Forschung of Germany, the Institut National de la Physique Nucleaire et de la Physique des Particules of France, the United Kingdom Engineering and Physical Sciences Research Council, Fundacao de Amparo a Pesquisa do Estado de Sao Paulo, Brazil, and the Russian Ministry of Science and Technology.

[1] For reviews and recent developments see *Quark Matter '99* [Nucl. Phys. **A661** (1999)].
[2] H. Sorge, Phys. Lett. B **402**, 251 (1997).
[3] J.-Y. Ollitrault, Phys. Rev. D **46**, 229 (1992).
[4] E877 Collaboration, J. Barrette *et al.,* Phys. Rev. C **55**, 1420 (1997).
[5] E895 Collaboration, C. Pinkenburg *et al.,* Phys. Rev. Lett. **83**, 1295 (1999).
[6] NA49 Collaboration, H. Appelshäuser *et al.,* Phys. Rev. Lett. **80**, 4136 (1998).
[7] NA49 Collaboration, A. M. Poskanzer and S. A. Voloshin, Nucl. Phys. **A661**, 341c (1999).
[8] WA98 Collaboration, M. M. Aggarwal *et al.,* Phys. Lett. B **403**, 390 (1997); M. M. Aggarwal *et al.,* Nucl. Phys. **A638**, 459c (1998).
[9] STAR Collaboration, K. H. Ackermann *et al.,* Phys. Rev. Lett. **86**, 402 (2001).
[10] J.-Y. Ollitrault, Nucl. Phys. **A638**, 195c (1998).

[11] X. N. Wang, Phys. Rev. C **63**, 054902 (2001).
[12] M. Gyulassy, I. Vitev, and X. N. Wang, Phys. Rev. Lett. **86**, 2537 (2001).
[13] D. Molnár and M. Gyulassy, e-print nucl-th/0102031.
[14] P. F. Kolb, P. Huovinen, U. Heinz, and H. Heiselberg, Phys. Lett. B **500**, 232 (2001).
[15] P. Huovinen, P. F. Kolb, U. Heinz, P. V. Ruuskanen, and S. A. Voloshin, Phys. Lett. B **503**, 58 (2001).
[16] NA44 Collaboration, I. G. Bearden *et al.,* Phys. Rev. Lett. **78**, 2080 (1997); NA44 Collaboration, N. Xu *et al.,* Nucl. Phys. **A610**, 175c (1996).
[17] EOS Collaboration, S. Wang *et al.,* Phys. Rev. Lett. **76**, 3911 (1996).
[18] E877 Collaboration, S. A. Voloshin, Nucl. Phys. **A638**, 455c (1998).
[19] STAR Collaboration, K. H. Ackermann *et al.,* Nucl. Phys. **A661**, 681c (1999).
[20] C. Adler *et al.,* e-print nucl-ex/0008005.
[21] A. M. Poskanzer and S. A. Voloshin, Phys. Rev. C **58**, 1671 (1998).
[22] STAR Collaboration, R. J. M. Snellings *et al.,* e-print nucl-ex/0104006.
[23] Minimum-bias corresponds to 0%–85% of the total measured cross section, deduced from the measured charged particle multiplicity [9], excluding the 15% most peripheral events. The total measured cross section is estimated to correspond to about 90% of the geometric cross section, with losses mainly due to vertex finding inefficiencies for the low multiplicity events.
[24] S. A. Voloshin, Phys. Rev. C **55**, 1630 (1997).
[25] P. Siemens and J. O. Rasmussen, Phys. Rev. Lett. **42**, 880 (1979).
[26] P. Huovinen, P. F. Kolb, and U. Heinz, e-print nucl-th/0104020.
[27] D. Teaney, J. Lauret, and E. V. Shuryak, Phys. Rev. Lett. **86**, 4783 (2001).